Journal of Alloys and Compounds 271–273 (1998) 363–366

Local structure of (U,Zr)Pd_3 by EXAFS

M. Akabori*, T. Ogawa, A. Itoh, H. Motohashi, H. Shiwaku

Japan Atomic Energy Research Institute, Tokai-mura, Naka-gun, Ibaraki-ken 319-11, Japan

---

Abstract

Measurements of the extended X-ray absorption fine structure (EXAFS) were used to determine the local configuration around uranium and zirconium atoms in (U,Zr)Pd_3 solid solutions. Interatomic distances and lattice constants from EXAFS and X-ray diffraction, respectively, are discussed in relation to the effect of addition of $ZrPd_3$ to UPd_3. The decrease in U–Pd distance with $ZrPd_3$ addition was appreciably smaller than the average M–Pd (M=U, Zr) distance of the solutions. The result suggests that the 5-f localized electronic structure of UPd_3 resists compression by the addition of $ZrPd_3$. © 1998 Elsevier Science S.A.

Keywords: Uranium alloy; Palladium alloy; EXAFS; Crystal structure; 5-f electrons

---

1. Introduction

A knowledge of the interaction of actinides with elements of the second row of Group VIII elements is important to understand the behavior of reactor fuels, in which type MX_3 compounds are formed where M is U and Pu and X is Ru, Rh and Pd [1]. These noble metal-actinide intermetallic compounds are characterized by large negative enthalpies of formation.

Studies of these actinide alloys and intermetallics are also informative for elucidating changing trends in 5-f electron bonding. In general, the 5-f electron nature in actinide compounds is influenced by the ligand. The localized state of 5-f electrons in UPd_3, that is, tetravalent f^2-configuration, is well known. UPd_3 adopts the $TiNi_3$ type hexagonal structure of the space group $P6_3/mmc$ with lattice spacings of $a_0=0.5769$ and $c_0=0.9640$ nm [2]. The $TiNi_3$ structure has atomic sites: 2 Ti_1 (0,0,0); 2 Ti_2 (1/3,2/3,1/4); 6 Ni_1 (1/2,0,0); 6 Ni_2 (0.833,0.666,1/4). The hexagonal structure is closely related to the $AuCu_3$ face-centered cubic structure and differs in the stacking sequence of layers (*abacabac* in the $TiNi_3$ structure, *abcabc* in the $AuCu_3$ structure). The nearest neighbors of uranium atoms in those structures are exclusively palladium atoms. All the interatomic distances in the $AuCu_3$ structure are the same. The $TiNi_3$ structure has two different interatomic distances at the nearest neighbors, which are 0.2885 and 0.2931 nm for UPd_3. The second-nearest neighbors of a uranium atom in UPd_3 are uranium atoms, where the interatomic distance of U–U is 0.4111 nm.

The molar volume of uranium in UPd_3 increases exceptionally at forming this compound because of localization of 5-f electrons, which are itinerant in pure uranium. UPd_3 is also the most thermodynamically stable intermetallic compound, because ΔH_f (the standard enthalpy of formation)$=-548$ kJ/mol [3]. By contrast, the molar volume of zirconium in $ZrPd_3$ having $\Delta H_f=-346$ kJ/mol [4] and the same structure, where the lattice spacings $a_0=0.5612$ and $c_0=0.9235$ nm [5], decreases significantly upon forming this compound.

X-ray absorption spectroscopy is a technique which can unambiguously examine the coordination around a particular element in a complex structure and the 5-f electron state of actinide systems. In this study, measurements of the extended X-ray absorption fine structure (EXAFS) were made to examine the local structure around uranium and zirconium atoms in (U,Zr)Pd_3 solid solutions.

2. Experimental

The intermetallics, UPd_3 and $ZrPd_3$, and their solid solutions, (U,Zr)Pd_3, containing 13, 25, 50 and 75 mol.% $ZrPd_3$ were prepared by arc-melting uranium, zirconium and palladium metals together in an argon atmosphere. The melting was repeated several times to ensure homogeneity of the buttons. Each button was wrapped with tantalum foils, sealed in evacuated quartz ampoules and annealed for

---

*Corresponding author. Tel.: +81 29 2825431; fax: +81 29 2826097; e-mail: akabori@popsvr.tokai.jaeri.go.jp

PII S0925-8388(98)00089-9

72 h at 1273 K. The buttons were very brittle and easily crushed to powder by an agate mortar in an argon glove box. The powders were annealed for 1 h at 973 K to remove lattice strains induced during crushing. However non-annealed powders were used for EXAFS measurements, since some faint diffraction lines arising from trace quantities of uranium oxide were observed.

X-ray diffraction at room temperature was performed in the range of 20–100° in 2θ using an X-ray diffractometer with Cu Kα radiation. Nine diffraction lines were analyzed with the Cohen's method to calculate the lattice parameters of $(U,Zr)Pd_3$.

The EXAFS measurements were performed in transmission geometry at the hard X-ray station BL-27 of the Photon Factory in the Institute of Materials Structure Science of the High Energy Accelerator Research Organization, Tsukuba, Japan, operating at an energy of 2.5 GeV and an average current of 200 mA. The radiation was monochromatized by a double-crystal Si (111) monochromator. The intensities of both incident and transmitted beams were monitored by two ion chambers in series. The instrumental resolution was better than 3.2 eV which was estimated from the FWHM of peaks on rocking curves measured at U-L_3 (17.167 keV) and Zr-K (17.998 keV) edges. Powder samples were supported between strips of adhesive tape. The sample thicknesses were ~35 and ~65 μm for UPd_3 and $ZrPd_3$, respectively, which were chosen to be $\mu t=2.6$ and $\Delta\mu t=1$, because the optimum μt to measure EXAFS is 2.6 on the basis of statistics, where μ is the total X-ray absorption coefficient and t is the sample thickness. All data were recorded at room temperature. The EXAFS monochromator was calibrated with respect to the energies at the absorption edges of UO_2 powder and Zr foil immediately before the $(U,Zr)Pd_3$ sample of interest.

3. Analysis

EXAFS data were analyzed in the conventional way with the computer program WinXAS version 2.4 by T. Ressler [6]. The interatomic distances were determined from fitting the inverse Fourier transform of the isolated contribution of interest shells on the R-space distributions to the EXAFS equation using theoretical back-scattering amplitudes and phase shift functions for the corresponding shells, which were calculated with the EXAFS analysis code, FEFF version 7 [7].

4. Results and discussion

The X-ray diffraction patterns of $(U,Zr)Pd_3$ solid solutions showed a single phase with a hexagonal structure. The lattice spacings are shown in Fig. 1 as a function of $ZrPd_3$ concentration. Both the lattice spacings of a and c decrease almost linearly with increasing $ZrPd_3$ content. It also shows that the decrease in the lattice spacings at the addition of $ZrPd_3$ is larger for c than for a.

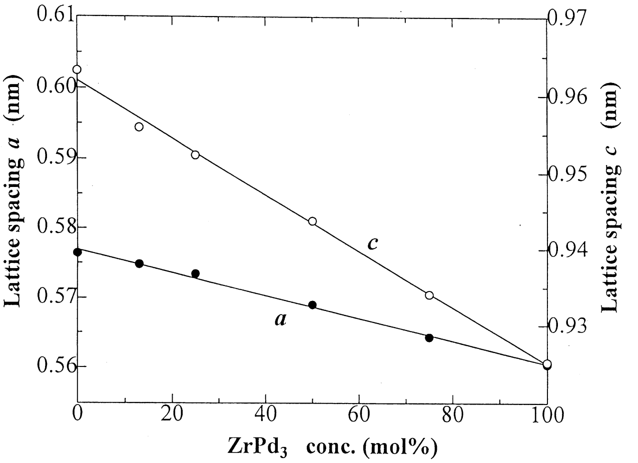

Fig. 1. Lattice spacings of $(U,Zr)Pd_3$ as a function of $ZrPd_3$ concentration.

Fig. 2 shows X-ray absorption spectra, $\ln(I_0/I)$, obtained from measurements on UPd_3, $ZrPd_3$ and $U_{0.5}Zr_{0.5}Pd_3$ near the U-L_3 and Zr-K absorption edges. The U-L_3 edge of UPd_3 can be clearly characterized by its high amplitude of the so-called white line, as compared to the Zr-K edge of $ZrPd_3$. The X-ray absorption near edge spectra (XANES) contains important information regarding the valence state, for uranium compounds [8]. The change of white-line position and its shape vaguely reflect the transition from 5-f localization to 5-f itinerancy. The white-line position of UPd_3 was in good agreement with that of tetravalent UO_2, suggesting that uranium atoms in UPd_3 adopt tetravalent configuration. For $(U,Zr)Pd_3$, the white-line position and its shape were not noticeably affected by the addition of $ZrPd_3$.

The k^3-weighted EXAFS oscillation of U-L_3 edge for

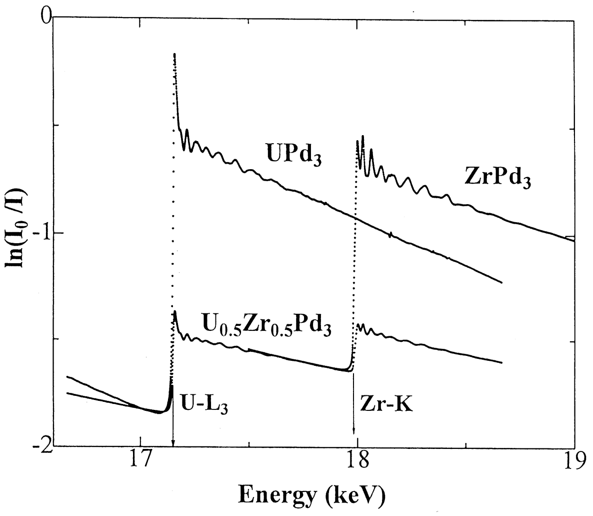

Fig. 2. EXAFS spectra of U-L_3 and Zr-K absorption edges for UPd_3, $ZrPd_3$ and $U_{0.5}Zr_{0.5}Pd_3$.

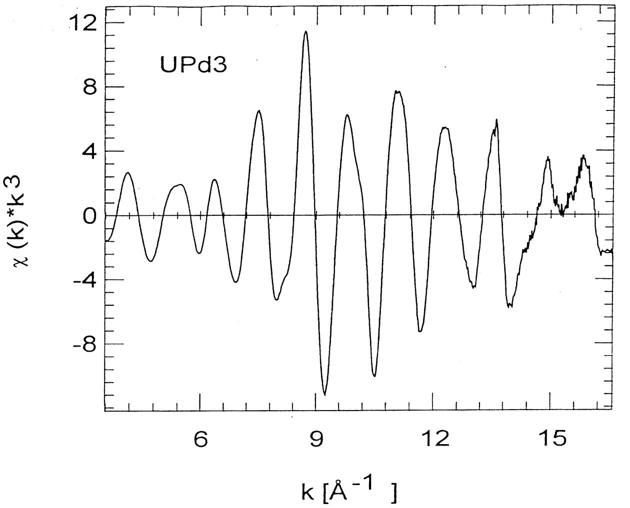

Fig. 3. k^3-weighted EXAFS oscillation of U-L_3 edge for UPd_3.

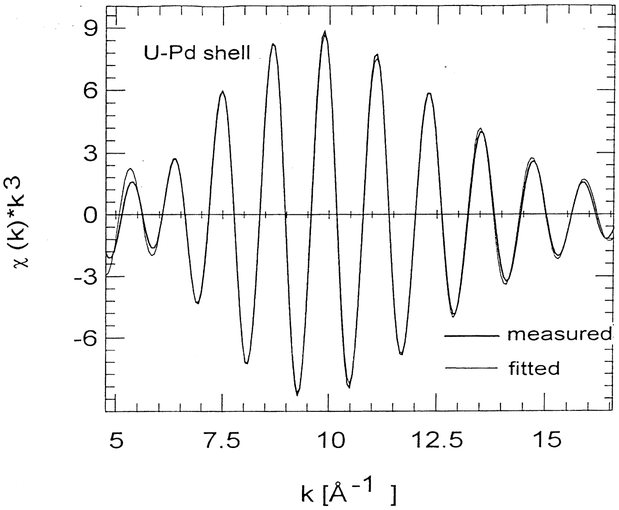

Fig. 5. Curve-fit to the U–Pd shell for UPd_3.

UPd_3, where k is the photoelectron wavevector, and its Fourier transform are shown in Fig. 3 and Fig. 4, respectively. As the Fourier transform is produced without consideration of the absorber and scatterer phase shifts for the backscattering atoms, the peaks are not expected to correspond exactly to the true interatomic distances. The first peak on the R-space distribution is attributed to a shell of nearest neighbor palladium atoms. The second peak is due to a shell of second-nearest uranium or zirconium. As shown in Fig. 4, the amplitude of the second peak is very small even for pure UPd_3 compared to that of the first peak. In the case of $U_{0.5}Zr_{0.5}Pd_3$, the second peak was almost extinguished. In this study, only the average interatomic distances of U–Pd and Zr–Pd were estimated from the first peaks on the R-space distributions of U-L_3 and Zr-K absorption edges, where the coordination number was assumed to be 12.

The first shell data regarding M–Pd in the $(U,Zr)Pd_3$ solutions were isolated by inverse transforming the Fourier transformed data over the R-space range corresponding to that shell. Analysis proceeded with fitting procedures using a least-square minimization routine and theoretical parameters, which were calculated with the FEFF code for model compounds of UPd_3 and $ZrPd_3$. The FEFF code was also tested on uranium dioxide as a well-known uranium compound, and the result obtained from fitting the EXAFS data was found to be in excellent agreement with the crystallographically determined values. The fit to the inverse transform of the first peak (U–Pd) on the R-space distribution for UPd_3 is shown in Fig. 5, indicating a successful refinement. The interatomic distances obtained from the curve-fitting and the lattice spacings are summarized in Table 1 and Fig. 6.

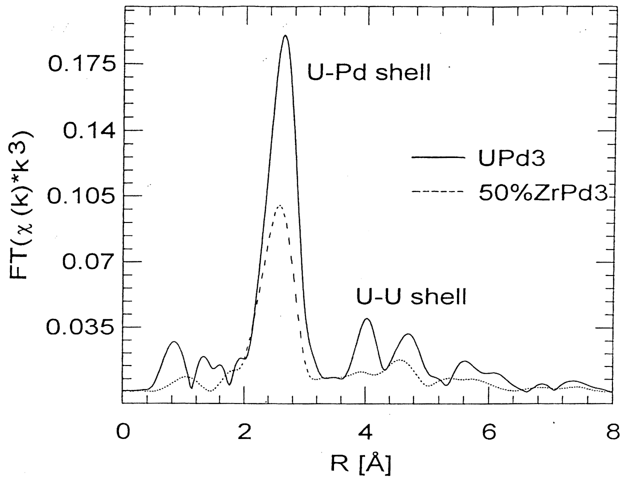

Fig. 4. R-space distributions of U-L_3 edge for UPd_3 and $U_{0.5}Zr_{0.5}Pd_3$.

The U–Pd interatomic distances by EXAFS are significantly larger than the average M–Pd distances obtained from the lattice spacings. On the contrary, the Zr–Pd distances are smaller. However, a good agreement exists between the average M–Pd distance by EXAFS and that by X-ray diffraction. If the valence state of uranium atoms in $(U,Zr)Pd_3$ was hexavalent, the U–Pd interatomic distance would become 0.284 nm, which was calculated from molar volumes of hexavalent U [9] and Pd, on the assumption that the UPd_3 structure adopts the close-packed

Table 1
The interatomic distances of M–Pd (M=U and Zr) obtained from EXAFS and X-ray diffraction

$ZrPd_3$ (mol.%)	EXAFS (nm)			M–Pd (nm) from X-ray diffraction	
	U–Pd	Zr–Pd	M–Pd	This work	Literature
0	0.2906		0.2906	0.2905	0.2908
13	0.2899	0.2850	0.2893	0.2892	0.2896[a]
25	0.2892	0.2844	0.2880	0.2884	0.2884[a]
50	0.2870	0.2835	0.2853	0.2861	0.2861[a]
75	0.2858	0.2823	0.2832	0.2835	0.2837[a]
100		0.2815	0.2815	0.2813	0.2814

[a] Assuming Vegard's law.

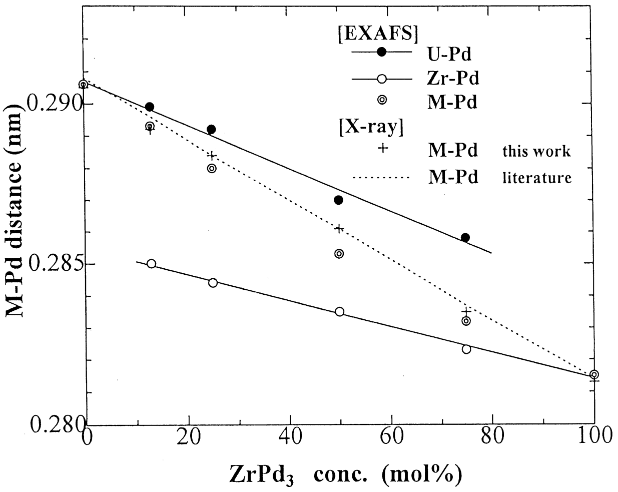

Fig. 6. Interatomic distances of U–Pd, Zr–Pd and average M–Pd (M=U and Zr) by EXAFS and X-ray diffraction.

$AuCu_3$ fcc structure, which is similar to coordination of palladium atoms around a uranium atom in the $TiNi_3$ structure. However, the result suggests that the 5-f localized electronic structure of uranium atoms, which is characteristic of UPd_3, tends to resist the compression by the addition of $ZrPd_3$ even at 75 mol.% $ZrPd_3$.

Acknowledgements

The authors would like to thank Drs. K. Kobayashi and N. Usami, the Institute of Materials Structure Science of High Energy Accelerator Research Organization, for useful discussion and guidance.

References

[1] J.L. Bramman, R.M. Sharpe, D. Thom, G. Yates, J. Nucl. Mater. 25 (1968) 201.
[2] T.J. Heal, G.I. Williams, Acta Cryst. 8 (1955) 494.
[3] G. Wijbenga, J. Chem. Thermodyn. 14 (1982) 483.
[4] S. Stolen, T. Matsui, K. Naito, J. Nucl. Mater. 173 (1990) 48.
[5] A.E. Dwight, P.A. Beck, Trans. AIME 215 (1959) 976.
[6] T. Ressler, J. Phys. IV 7(4) (1997) C2–C269.
[7] S.I. Zabinsky, J.J. Rehr, A. Ankudinov, R.C. Albers, M.J. Eller, Phys. Rev. B 52 (1995) 2995.
[8] G. Kalkowski, G. Kaindl, W.D. Brewer, W. Krone, Phys. Rev. B 35 (1987) 2667.
[9] W.H. Zachariasen, J. Inorg. Nucl. Chem. 35 (1973) 3487.